Chemically Introduced Disorder Effects on the Critical Current Density and Pinning Mechanisms of $YBa_{2-x}Sr_xCu_3O_{7-\delta}$

R. F. Lopes , V. N. Vieira, F. T. Dias, P. Pureur, , J. Schaf, , M. L. Hneda, and J. J. Roa

***Abstract*— We report on isotherm (*T* = 77.5 K) DC magnetization hysteresis loops of a series of $YBa_{2-x}Sr_xCu_3O_{7-\delta}$ (x = 0, 0.02, 0.1, 0.25 and 0.37) single crystals with the purpose of studying the influence of chemically introduced site disorder on the $YBa_2Cu_3O_{7-\delta}$ critical current density, *$J_c(B,T)$* and normalized pinning force density, *f(h)*. The Sr ion chemical disorder is inserted at $YBa_2Cu_3O_{7-\delta}$ structure by lattice distortion. Transmission electronic microscopy (TEM) of the doped samples shows a structure constituted by a high density of twins, probably, decorated by many small precipitates. The *$J_c(B,T)$* transported by the doped samples with x ≤ 0.10 is higher than that transported by the $YBa_2Cu_3O_{7-\delta}$ pure sample. In contrast, the *$J_c(B,T)$* transported by the doped samples with x > 0.10 is significant and systematically lower than that transported by the undoped sample. The analysis of the *f(h)* plots indicates, in the light of Dew Hughes model, that the preponderant pinning mechanism of $YBa_{2-x}Sr_xCu_3O_{7-\delta}$ single crystals with x ≤ 0.10 is the core normal point type. However to the samples with x > 0.10, the *f(h)* analyses indicates that the preponderant pinning mechanism undergoes a crossover from the core normal point type to the core normal surface type. This crossover of pinning mechanism dynamics could be appointed as the possible reason of the decrease of the *$J_c(B,T)$* observed in the samples with x > 0.10.**

***Index Terms* — Chemical doping, Critical Current Density, Pinning Mechanisms, Single crystals and $YBa_{2-x}Sr_xCu_3O_{7-\delta}$**

I. Introduction

The application of chemical substitution in the high temperature superconductors (HTSC) structure has been showed to be an efficient tool to promote the enhancement of the $J_c(B,T)$ transported by these materials and therefore collaborating to the development of their technological potential. The introduction of flux pinning centers by chemical substitutions in the HTSC structure can be done in a such way that allows classify and quantify the flux pinning mechanism efficiently. The enhancement of the $J_c(B,T)$ is reported to $YBa_2Cu_3O_{7-\delta}$ single crystals when Y, Ba and Cu sites are partially substituted by Ca, Sr and Zn atoms, respectively [1]-[8]. However, scarce and not concluding are the physical interpretations, presented in the literature, which focus on how the amount of chemical element applied as dopant affects the $YBa_2Cu_3O_{7-\delta}$ pinning mechanisms and consequently the $J_c(B,T)$ transported by this material [3]-[7].

The Sr ion disorder is introduced at $YBa_2Cu_3O_{7-\delta}$ structure by lattice distortion [9]-[11]. The solubility of the Sr atoms at Ba site is almost 50% [9]-[11] and the enhancement of the $J_c(B,T)$ is observed to Sr concentrations lower than 6% (x ≤ 0.12) [2], [3], [5]. Some authors point out as responsible for the enhancement of $J_c(B,T)$ transported by the $YBa_{2-x}Sr_xCu_3O_{7-\delta}$ single crystals the configuration of a physical structure constituted by a high density of twin planes decorated by, probable, Sr atom precipitates [2], [3]. However, a recent AFM study made in a $YBa_{1.75}Sr_{0.25}Cu_3O_{7-\delta}$ single crystal shows that Sr doping concentrations up to approximately 12.5% corroborates to the enlargement of porosity and roughness of the $YBa_2Cu_3O_{7-\delta}$ single crystal surface [13] witch, probably, affects negatively the efficiency of the flux pinning mechanism of $YBa_2Cu_3O_{7-\delta}$ single crystal.

Motivated by the last considerations, we report on isotherm DC magnetization measurements, at T = 77.5 K, with H // c, of a series of $YBa_{2-x}Sr_x Cu_3O_{7-\delta}$ (x = 0, 0.02, 0.1, 0.25 and 0.37) single crystals with the aim of studying the role of the chemically introduced disorder on $J_c(B,T)$ and $f(h)$ of the $YBa_2Cu_3O_{7-\delta}$ superconductor.

II. Experiments and Discussion

The $YBa_{2-x}Sr_xCu_3O_{7-\delta}$ (x = 0, 0.02, 0.1, 0.25 and 0.37) single crystals, labeled as ScY, ScSr002, ScSr01, ScSr025 and ScSr037 respectively, were prepared by self flux method. More details about preparation method and single crystals fundamental superconducting properties characterization are expressed in the references 9 and 10. The single crystals structure was previously analyzed by X ray diffraction (XRD),

August 11,2015.
This work was partially supported by CAPES and CNPq Brazilian scientific agencies.

Rovan Fernandes Lopes, (R. F. Lopes), (corresponding author) is with Instituto de Física, UFRGS, 91501-970, Porto Alegre, Brazil (e-mail: rovanfl@gmail.com)
Paulo Pureur (P. Pureur), Jacob Schaf (J. Schaf), and Marlon Luis Hneda (M. L. Hneda) are with Instituto de Física, UFRGS, 91501-970, Porto Alegre, Brazil (e-mail: ppureur@if.ufrgs.br, schaf@if.ufrgs.br and mlhneda@if.ufrgs.br).
Valdemar das Neves Vieira (V. N. Vieira) and Fábio Teixeira Dias (F. T. Dias) are with Instituto de Física e Matemática, UFPEL, 96010-610, Pelotas, Brazil (e-mail: vdnvieira@gmail.com and diasft@gmail.com)
Joan Josep Roa (J. J. Roa) is with Department of Materials Science and Metallurgical Engineering, University of Barcelona, 08028, Barcelona, Spain (e-mail: joan.josep.roa@upc.edu)

This article has been accepted for publication in a future issue of this journal, but has not been fully edited. Content may change prior to final publication. Citation information: DOI 10.1109/TASC.2016.2525927, IEEE Transactions on Applied Superconductivity

polarized light microscopy (PLM) and transmission electron microscopy (TEM) [9], [10]. The XRD diffractogram of the doped samples showed the Y123 orthorhombic structure with c lattice parameter in agreement with those reported in the literature for others well oxygenated Sr doped samples [10]-[12]. The PLM and TEM results identify in the doped samples the presence of a high density of twin planes, possibly, decorated by Sr atom precipitates.

The Fig. 1 a) and b) were obtained from ScSr025 by TEM analysis. In Fig. 1 a) the existence of twin planes is highlighted. The Fig. 1 b) represents the amplification of a twin plane region of Fig. 1 a). The presence of black spots (red circles), probably, is associated with the existence of Sr atoms precipitates at ScSr025 structure.

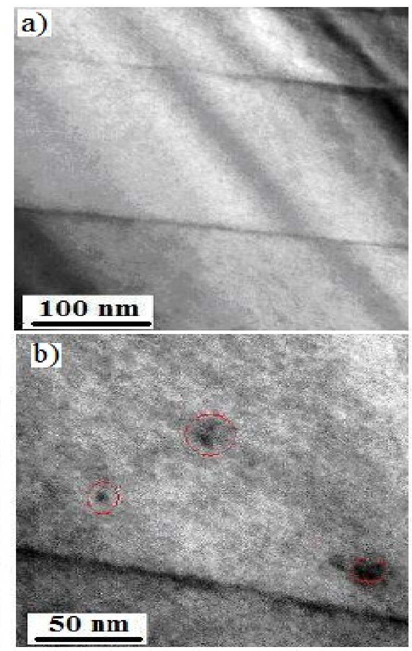

Fig 1 – The TEM images of ScSr025 sample where the existence of twin planes decorated by, possibly, Sr atoms precipitates is put in evidence.

Isothermal DC magnetization measurements of our samples were done at T = 77.5 K with a SQUID magnetometer when magnetic fields up to 5T were applied parallel to c crystallographic axis of the samples. Fig. 2 displays the magnetization hysteresis loops, $M(B)$ of our samples with T = 77.5 K. The SPM arrow identifies the presence of the second peak magnetization (SPM) [2]-[4], [8], [14], [18], [19], and the $B_{IRR}(T)$ arrow defines the irreversible magnetic filed [2], [8]. The $B_{IRR}(T)$ data obtained from $M(B)$ measurements of Fig 1 matches, considering the experimental resolution, with those reported in the references [9] and [10] to the magnetic irreversibility line (IML), obtained from $M(T)$ measurements, to the same $YBa_{2-x}Sr_xCu_3O_{7-\delta}$ (x = 0; 0.10; 0.25 and 0.37) single crystals applied at this work. The B-T plots of the $B_{irr}(T)$ data of our samples are fitted by $B_{irr}(T) \approx [1- T(B)\ T_{irr}(B = 0)^{-1}]^{1.5}$ power law which is supported by giant flux creep scenario. The correspondence between the $T_{irr}(B)$ data, determined from $M(T)$ measurements, and the $B_{IRR}(T)$ data, obtained from $M(B)$ measurements, collaborates to attenuate the experimental uncertain in the determination of the reduced field, $h = B/B_{irr}$.

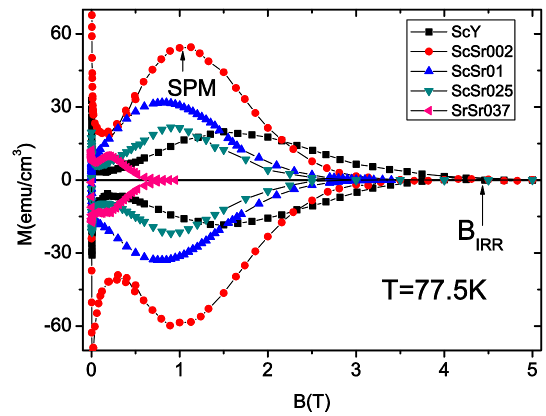

Fig 2 – The $M(B)$ plots of ScY, ScSr002, ScSr01, ScSr025 and ScSr037 single crystals at T = 77.5 K. The arrows define the second peak magnetization (SPM) and the magnetic irreversible field, $B_{IRR}(T)$.

The $J_c(B,T)$ data highlighted in the Fig. 3 was calculated from the application of the extended Bean critical model [5]-[8] to the magnetization hysteresis loops of Fig. 2.

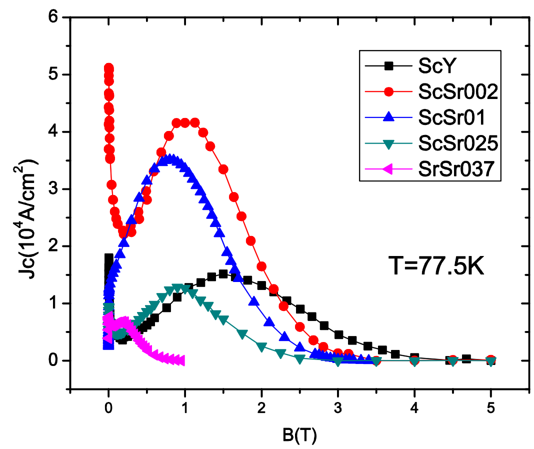

Fig 3 – The $J_c(B,T)$ plots for ScY, ScSr002, ScSr01, ScSr025 and ScSr037 single crystals at T = 77.5 K.

The SPM in the $M(B)$ plots marks approximately the maximization of the flux pinning potential resulting in higher $J_c(B,T)$ values. It is important to highlight that for $B \leq 1.6$ T the Sr doped samples ScSr002 and ScSr01 transport higher $J_c(B,T)$ values than that transported by the ScY sample. The maximum values of $J_c(B,T)$ transported by the ScSr002, ScSr01 samples, in the presence of applied magnetic field, were $4.2 \pm 0.7\ 10^4$ Acm^{-2}, for $B \sim$ 1T and $3.5 \pm 0.7\ 10^4$ Acm^{-2}, for $B \sim$ 0.8T, respectively. In contrast, the maximum values of $J_c(B,T)$ transported by the ScSr025 and ScSr037 samples are systematically lower than that transported by the ScY sample [3], [5].

The pinning force, $F_P(B,T)$ of the samples was calculated from the application of the equation (1) [6]-[8] to the $J_c(B,T)$ data showed in Fig. 3.

This article has been accepted for publication in a future issue of this journal, but has not been fully edited. Content may change prior to final publication. Citation information: DOI 10.1109/TASC.2016.2525927, IEEE Transactions on Applied Superconductivity

$$\vec{F}_p = \vec{J}_C \, x \, \vec{B} \qquad (1)$$

The $F_P(B,T)$ behavior, as function of the Sr concentration, (not displayed at the text) showed a profile very similar to that reveled by the $J_c(B,T)$ in Fig. 3, where the ScSr002 sample showed the best performance.

The normalized pinning force density, $f = F_P/F_{P,max}$ (where $F_{P,max}$ corresponds to the upper $F_P(B,T)$ data) versus the reduced field, $h = B/B_{irr}$ plots is applied as an efficiently tool to identify and distinguish the contribution of the different pinning mechanisms to the behavior of $J_c(B,T)$ [1], [6], [8], [14], [15].

Fig. 4, below, shows the behavior of $f(h)$ plots obtained for our samples to $T = 77.5$ K.

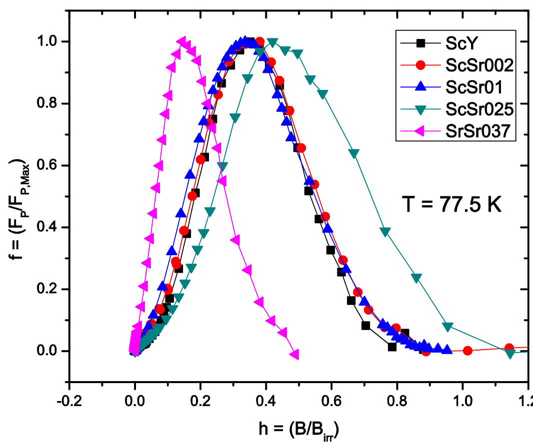

Fig. 4 – $f(h)$ ($f = F_p/F_{p,Max}$ and $h = B/B_{irr}$) plots of ScY, ScSr002, ScSr01, ScSr025 and ScSr037samples at $T = 77.5$ K.

The pinning mechanisms dynamics of our samples displayed in the Fig. 4 are directly associated to the behavior of $J_c(B,T)$ showed in the Fig. 3.

We apply the Dew-Hughes (D-H) model [15], [16] to evaluate the role of Sr chemically introduced disorder on the flux pinning mechanisms properties and $J_c(B,T)$ transported by the $YBa_2Cu_3O_{7-\delta}$ single crystals. Fig. 5 shows the $f(h)$ plots where a series of pinning mechanisms functions are provided by the application of the D-H model. The D-H model proposes that the flux pinning mechanisms of a type II superconductor can be analyzed from the application of a universal pinning scale function of the type stipulated in the equation 2.

$$f(h) = Ah^p (1-h)^q \qquad (2)$$

In the equation (2), A is a numerical parameter, p and q are fitting parameters related to the geometric characteristics of the pinning centers. For the case of HTSC the appropriate scaling field applied in the reduced field h of equation (2) is the $B_{IRR}(T)$ instead $B_{C2}(T)$, which is specifically used to the case of conventional type II superconductors [1], [6], [8], [14].

The types of pinning mechanisms showed in the Fig. 5 are classified as normal (N) and Δk (delta k).

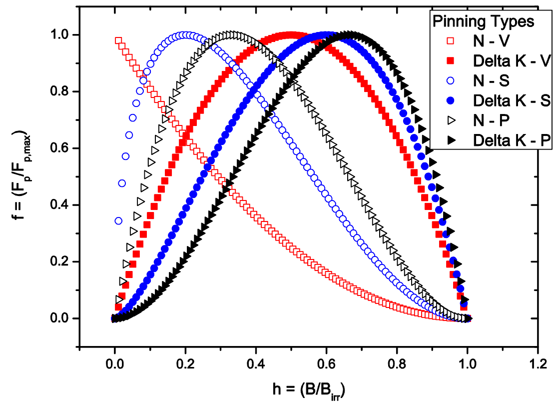

Fig 5 – The different flux pinning mechanisms predicted by the Dew-Hughes model in ($f = F_p/F_{p,Max}$ and $h = B/B_{irr}$) plots adapted from reference [15].

The N pinning is related to the non superconducting regions while the Δk pinning is connected to the regions with weak superconductivity and/or displaying k, Ginsburg-Landau parameter, spatial variations. In contrast, the letters p (point), s (surface) and v (volumetric) in the caption of Fig. 5 are associated to the pinning geometric shape compared to the inter-flux vortex distance.

The D-H pinning mechanisms functions have their better physical performance when they are successful in fit the maximum of $f(h)$ data [14],[15]. At this scenario the pinning mechanisms are classified in terms of a reduced field h_0 which is defined as the h axis value that marks the maximum of the $f(h)$ function [14], [15].

In this way, we decided to apply the criterion described in the previous paragraph to analyze and classify the main flux pinning mechanism of our samples by contrasting the $f(h)$ plots in Fig. 4 to those in Fig. 5. The h_0 value estimated for the samples takes into account the possible uncertainties in the calculation of h ($h = B/B_{irr}$) introduced from $B_{irr}(T)$ data.

It is possible to confirm that the main pinning mechanism of ScY ($h_0 = 0.35 \pm 0.02$), ScSr002 ($h_0 = 0.34 \pm 0.02$) and ScSr01 ($h_0 = 0.34 \pm 0.02$) samples is the core normal point type ($h_0 = 0.33$). It is in agreement with other results reported by the literature to $YBa_2Cu_3O_{7-\delta}$ single crystals [1], [8], [17]. Similarly to the ScSr025 ($h_0 = 0.42 \pm 0.05$) and ScSr037 ($h_0 = 0.17 \pm 0.05$) samples, the main pinning mechanism identified is the core Δk volume type ($h_0 = 0.5$) to the ScSr025 sample and core normal surface type ($h_0 = 0.2$) to the ScSr037 sample.

We believe that the core normal point pinning mechanism, observed for the samples with $x \leq 0.1$, is originated from the point like structural defects, specially, oxygen vacancies, in the pure sample, and defects of Sr inter-site atoms, in the case of ScSr002 and ScSr01 samples. The higher $J_c(B,T)$ transported by the doped samples with $x \leq 0.1$, when compared to that transported by the pure one, could be associated to the fact that the low concentration of Sr atoms precipitates produces a flux pinning potential stronger than that produced by the oxygen vacancies in the pure sample.

For ScSr037 is possible to notice that the core normal surface pinning mechanism is associated to the lower $J_c(B,T)$ values transported by this sample. The activation of this mechanism is possibly connected to the high addition of the Sr atoms content not absorbed by the $YBa_2Cu_3O_{7-\delta}$ structure. This could cooperate to the nucleation of a large number of Sr clusters and distorted regions at sample structure.

On the other hand, as well as ScSr037, the ScSr025 transports a $J_c(B,T)$ lower than that transported by the pure sample. When compared with others Sr doped samples its $f(h)$ curve decreases smoothly as the applied magnetic field is increased. This behavior is the signature of the core Δk volumetric pinning mechanism whose preponderance in the $f(h)$ curve of ScSr025 could be interpreted in two ways. The first one, as a pinning mechanism crossover between the core normal point and surface types as the amount of Ba atoms, partially substituted by Sr atoms in the $YBa_2Cu_3O_{7-\delta}$ single crystal, increases from $0 < x \leq 0.37$. The other one stands to the fact that the nucleation of weak ScSr025 superconductor regions are "stronger" than those presented in the others samples of this work and, in this scenario, they have a higher critical field which collaborates to the predominance of Δk pinning mechanism in the vicinity of h_0 at $f(h)$ plot.

It is interesting to notice that the development of pinning mechanisms dynamics of our doped samples, as function of Sr doping, from the point like type to the surface like type is promoted by the achieving of the volumetric like type as the applied magnetic field is increased. It could be justified due to the reduction of the inter-vortex distance as the applied magnetic field is augmented [15]. This fact could explain the reduction in the width of the $f(h)$ curve, showed in the Fig. 4, as the reduced field, h enhances.

Aside the reliability of the D-H model, in the low reduced magnetic field regime, it is interesting to notice that the pinning mechanisms of low Sr doped samples undergo a crossover from Δk surface type to Δk volumetric type, achieving the normal point type as the applied magnetic field approach to the h_0. This behavior in the $f(h)$ curves could be justified due to the activation of a field induced pinning mechanism.

III. CONCLUSION

The isotherm dc magnetization hysteresis loops, at T = 77.5 K, of a series of $YBa_{2-x}Sr_xCu_3O_{7-\delta}$ (x = 0, 0.02, 0.1, 0.25 and 0.37) single crystals showed the SPM in the $M(B)$ curves of all the studied samples. In particular, we suggest, in agreement with the authors of references [18], [19], that the presence of the SPM of our undoped single crystal probably is connected to the inhomogeneous distribution of the oxygen content at the structure of this sample. In the case of the Sr doped single crystals, we agree with the interpretation of Saito et al [3], which suggest that the Sr clusters, in the lattice structure of the single crystals with $x \leq 0.1$, are responsible for the enhancement of flux pinning properties and consequently to the higher $J_c(B,T)$ transported by those samples. According to the $f(h)$ plots analysis, the higher $J_c(B,T)$ transported by doped samples with $x \leq 0.1$ is connected to the dominance of the core normal point pinning mechanism. In contrast, the lower $J_c(B,T)$ transported by doped samples with $x > 0.1$ is connected to crossover of pinning mechanism to core normal surface type. In summary, the nucleation of the possible clusters of Sr atom precipitates at structure of the $YBa_2Cu_3O_{7-\delta}$ single crystals is responsible to the enhancement of flux pinning properties and consequently increasing of the $J_c(B,T)$ transported by those samples.

REFERENCES

[1] K. Rogacki, B. Dabrow and O. Chmaissem,"Increase of critical currents and peak effect in Mo-substituted $YBa_2Cu_3O_{7-\delta}$," *Phys Rev B*, vol. 73, no. 22, pp. 224518-1-224518-11, Jun. 2006.
[2] H. Küpfer, A. A. Zhukov, A. Will, W. Jahn, R. Meier-Hirmer, Th. Wolf, V. I. Voronkova, M. Kläser, and K. Saito, "Anisotropy in the irreversible behavior of pointlike defects and twins in $YBa_2Cu_3O_{7-\delta}$ single crystals with a peak effect" *Phys Rev B*, vol. 54, no. 1, pp. 644-655, Jul. 1996.
[3] K. Saito, H.-U. Nissen, C. Beeli, T. Wolf, W. Schauer, and H. Küpfer, "Influence of Sr doping on twin-wall structure and flux pinning of $YBa_2Cu_3O_{7-\delta}$ single crystals," *Phys Rev B*, vol. 58, no. 10, pp. 6645-6649, Sep. 1998.
[4] V. N. Vieira and J. Schaf, "Influence of Sr doping on the second magnetization peak and the critical current density of $YBa_2Cu_3O_{7-\delta}$ single crystals," *Physica C: Superconductivity*, vol. 408-410, pp. 533-534, Aug. 2004.
[5] J. Shimoyama, Y. Tazaky, Y. Ishii, T. Nakashima, S. Horii and K. Kishio, "Improvement of Flux Pinning Properties of RE123 Materials by Chemical Doping," *Journ. of Phys.: Conf. Series*, vol. 43, no. 1, pp. 235-238, Jun. 2006.
[6] Z. H. Wang, H. Zhang, J. Gao, T. Yang, L. Qiu and X. X. Yao, "K-doping induced peak effect in melt-textured grown $YBa_{2-x}K_xCu_3O_y$ crystals" *Supercond. Sci. Technol*., Vol. **15**, no 12, pp. 1766-1770, Dec. 2002.
[7] Y. Ishii , Y. Tazaki, T. Nakashima, J. Shimoyama, S. Horii and K. Kishio, "Enhanced flux pinning properties of RE123 crystals by dilute impurity doping for Cu–O chain," *Physica C,* vol. 460-462, no. 2, pp. 1345-1346, Sept. 2007
[8] M. Hussain, S. Kuroda and K. Takita, "Peak effect observed in Zn doped YBCO single crystals," *Physica C,* vol. 297, no. 3-4, pp. 176-184, Mar 1998.
[9] V. N. Vieira and J. Schaf, "Anisotropic irreversibility of the Abrikosov and Josephson flux dynamics in $YBa_{2-x}Sr_xCu_3O_{7-\delta}$ single crystals: Bose-glass and vortex-glass features," *Phys. Rev. B*, vol. 65, no. 14, pp. 144531-1-144531-9, April 2002.
[10] V. N. Vieira and J. Schaf, "Bose-glass, vortex-glass and superconducting-glass properties in Sr doped YBaCuO single crystals," *Physica C*, vol. 384, no. 4, pp. 514-524, Feb. 2003.
[11] M. Kakihana, S.-G. Eriksson, L Börjesson, L.-G. Johansson, C. Ström and M. Käll, "Charge-transfer and compression effects of isomorphous substitutions in $YBa_2Cu_3O_7$," *Phys. Rev. B*, vol. 47, no 9, pp. 5359-5366, March 1993.
[12] *F.* Licci, A. Gauzzi, M. Marezio, G. P. Radaelli, R. Masini and C. Chaillout-Bougerol, "Structural and electronic effects of Sr substitution for Ba in $Y(Ba_{1-x}Sr_x)_2Cu_3O_w$," *Phys. Rev. B*, vol. 58, no. 22, pp. 15208 – 15217, Dec. 1998.
[13] J. J. Roa G. Oncins, F.T. Dias, V.N. Vieira, J. Schaf, M. Segarra, "AFM as an alternative for Young's modulus determination in ceramic materials in elastic deformation regime," *Physica C,* vol. 471, no. 17-18, pp. 544-548, Sep. 2011.
[14] M. R. Koblischka, A. J. J. Van Dalen, T Higuchi, S. I. Yoo and M. Murakami, "Analysis of pinning in $NdBa_2Cu_3O_{7-\delta}$ superconductors," *Phys. Rev. B*, vol. 58, no. 5-1, pp. 2863-2867, Aug. 1998.
[15] D. Dew-Hughes, "Flux pinning mechanisms in type II superconductors," *Philos. Mag.,* vol. 30, no. 2, pp. 293-305 Mar. 1974.
[16] E. J. Kramer, "Scaling laws for flux pinning in hard superconductors," *J. Appl. Phys*., vol. 44, no. 3, pp. 1360-1370, March. 1973.
[17] J. N. Li, F. R. De Boer, L. W. Roeland, M. J. V. Menken, K. Kadowaki, A. A. Menovsky, J. J. M. Franse and P. H. Kes, "High-field magnetization of single-crystalline $YBa_2Cu_3O_7$," *Physica C*, vol. 169, pp. 81- 86, no. 1-2, Jul. 1990.
[18] H. Kupfer, Th. Wolf, C. Lessing, A. A. Zhukov, X. Lançon, R. Meier-Hirmer, W. Schauer and H. Wühl, "Peak effect and its evolution from oxygen deficiency in $YBa_2Cu_3O_{7-\delta}$ single crystals," *Phys. Rev. B,* vol 58, pp. 2886-2894, Aug. 1998.
[19] L. Klein E. R. Yacoby, Y. Yeshurun, A. Erb, G. Müller-Vogt, V. Breit and H. Wühl, "Peak effect and scaling of irreversible properties in untwinned Y-Ba-Cu-O crystals," *Phys. Rev. B*, vol. 49, no. 6, pp. 4403-4406, Feb. 1994.